

# SIZE EFFECT IN MULTIAXIAL DOUBLE PUNCH TESTS ON STEEL FIBRE REINFORCED CONCRETE CUBES

MINU LEE<sup>\*</sup>, TOMISLAV MARKIĆ<sup>\*</sup>, JAIME MATA-FALCÓN<sup>\*</sup>, ALI AMIN<sup>†</sup> AND  
WALTER KAUFMANN<sup>\*</sup>

<sup>\*</sup>ETH Zürich

Zürich, Switzerland

e-mail: [{lee, markic, mata-falcon, kaufmann}@ibk.baug.ethz.ch](mailto:{lee, markic, mata-falcon, kaufmann}@ibk.baug.ethz.ch)

<sup>†</sup>The University of Sydney

Sydney, Australia

e-mail: [ali.amin@sydney.edu.au](mailto:ali.amin@sydney.edu.au)

**Key words:** Steel Fibre Reinforced Concrete, Size Effect, Multidirectional Test, Double Punch Test.

**Abstract:** Test methods used to characterize steel fibre reinforced concrete (SFRC) at the material constitutive level continue to be a topic of discussion in the scientific community. The principal aim of these tests, as is required for input into physical models to describe structural behaviour, is to gather the residual or post-cracking response of the SFRC. Typically, this response is derived following an inverse analysis of flexural prism tests. However, it has been suggested that the anisotropy of the material due to the dispersion and orientation of the fibres cannot be accounted for in these tests. Multiaxial double punch tests have been proposed to overcome these issues. However, to the authors' knowledge, no attempt has been made to quantify the size effect in this test set-up, nor to study whether a sufficiently high amount of fibres can mitigate this effect. To this end, this paper presents preliminary findings on an experimental campaign investigating the size effect in multiaxial double punch tests on SFRC cubes. In this investigation, the specimen size varied from 75<sup>3</sup> to 600<sup>3</sup> mm<sup>3</sup>, covering a range of approximately 5 to 40 times the maximum aggregate size ( $D_{\max} = 16$  mm). The supplied fibre dosages ranged from 0-1% by vol. It is found that there was a pronounced size effect with respect to the cracking load of the cubes, which appears to be in good agreement with theoretical predictions. Further examinations are currently being carried out to quantify the size effect in the post-cracking phase of the tested SFRC specimens.

## 1 INTRODUCTION

The principal purpose of laboratory material testing is to provide data from which material properties required for design of structural elements can be accurately established. For the design of steel fibre reinforced concrete (SFRC), the most important characteristic of the material is its post-cracking residual tensile strength. Prior to cracking, the contribution of the fibres to the principal tensile strength of concrete is mostly

negligible. For a fibre to be effectively engaged in resisting tension, a small crack opening must occur to activate the fibre-matrix bond [1]. The material constitutive response of SFRC is typically determined either from uniaxial tension tests or following an inverse analysis of flexural prism or round panel tests [2]. However, it has been suggested that the anisotropy of the material due to the dispersion and orientation of the fibres are unable to be accounted for in these tests [3]. An attempt to

overcome this limitation is to test specimens cut out in different directions from a larger cuboid. However, this procedure is too expensive in time and labour to conduct in routine testing.

The double punch test on concrete cylinders was first proposed by Chen in 1970 [4]. This test offered an alternative to the split cylinder (also known as the Brazilian test) in determining the tensile strength of plain concrete. In this relatively simple and efficient test, a concrete cylinder is placed vertically between the loading platens of a testing machine and is compressed by two steel punches placed parallel to the top and bottom planes. These tests are attractive in that they do not confine failure of the specimen to a predefined plane and therefore the results are subject to a relatively low amount of scatter as highlighted by Marti [5], who investigated the size effect of plain concrete using this test on 42 specimens.

About a decade ago, Molins et al. [6] proposed to use double punch tests on cylinders for characterising the post-peak behaviour of SFRC. However, such tests cannot account for the anisotropy of SFRC caused by the distribution and, more importantly, the orientation of the fibres within the concrete. In order to overcome this drawback, Pujadas et al. [3] introduced the multidirectional double punch test on cubic SFRC specimens. These tests are relatively simple to perform and, at the same time, allow accounting for the influence of fibre orientation by testing the cubes at different orientations with respect to the casting direction. Hence, the double punch test is particularly suitable for larger test campaigns on specimens of different size, as is required for studying the size effect. As in all failures that result from cracking of concrete, a size effect must be expected [7], [8]. The size effect in SFRC at the structural level has received some research attention [9]–[11]. In these studies, it was found that the influence of size effect in shear critical large-scale beams may not be fully mitigated by the addition of fibres to the mix. However, to the authors’

knowledge, no attempt has been made to quantify this effect at the material level by using the multidirectional double punch test, nor to study whether a sufficiently high amount of fibres is able to alleviate this effect. This is the focus of this study, and first results are reported in this paper.

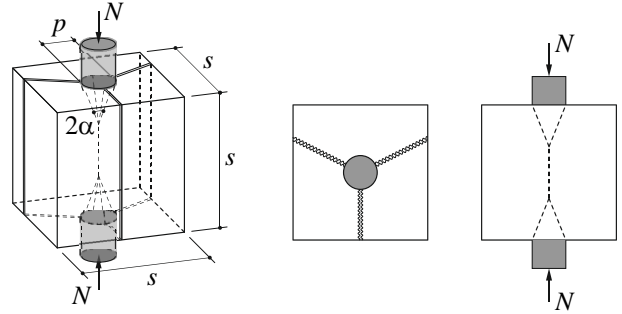


**Figure 1:** Principle of multidirectional double-punch test and typical failure mode: (a) Isometric view with geometry; (b) top view; (c) section.

## 2 EXPERIMENTAL CAMPAIGN

### 2.1 Specimens, materials and casting

An extensive experimental program was conducted to investigate the size effect in multidirectional double punch tests (see Figure 1) on SFRC cubes. A total of 54 SFRC cubes of varying sizes ranging from a side length of 75 mm to 600 mm were manufactured and tested to failure. The steel fibres used in this study were the Dramix 3D 65/35 fibres. The fibres were 0.55 mm in diameter and 35 mm long and had an ultimate notional tensile strength of 1350 MPa. Three fibre volumetric dosages were adopted, i.e.  $\rho_f = 0, 40$  and  $80 \text{ kg/m}^3$  (corresponding to 0, 0.5 and 1.0% by vol., respectively). An overview of the test specimens investigated is presented in Table 1.

The concrete strength class used was C25/30, with a maximum aggregate size of  $D_{\max} = 16 \text{ mm}$ . The concrete was provided to the testing laboratory without the fibres in the mix. In order to minimize variations in the concrete properties for all specimens (aside of the fibre content), the total required concrete volume for all specimens was delivered to the laboratory by one concrete mixer truck obtained from a local supplier.

**Table 1:** Properties of test specimens and cracking load.

fibre content [kg/m <sup>3</sup> ]			size [mm]	loading direction	cast   cut	cracking load $N_{cr}$ [kN]		
00	40	80	75	H	cast	31.5	29.6	25.0
00	40	80	75	V	cast	28.9	31.6	29.4
–	40	80	75	H	cut	–	34.2	31.8
–	40	80	75	V	cut	–	39.6	35.3
00	40	80	106	H	cast	65.8	58.9	66.6
00	40	80	106	V	cast	66.3	61.9	65.4
–	40	80	106	H	cut	–	59.6	56.3
–	40	80	106	V	cut	–	73.9	72.4
00	40	80	150	H	cast	125.2	116.6	129.4
00	40	80	150	V	cast	131.7	137.6	157.3
–	40	80	150	H	cut	–	126.7	114.6
–	40	80	150	V	cut	–	142.5	141.1
00	40	80	212	H	cast	268.2	242.9	210.6
00	40	80	212	V	cast	260.2	256.3	312.8
00	40	80	300	H	cast	470.8	427.3	442.0
00	40	80	300	V	cast	460.2	496.1	515.8
00	40	80	424	H	cast	863.7	691.5	752.4
00	40	80	424	V	cast	865.0	895.9	923.1
00	40	80	600	H	cast	1724.2	1347.7	1603.3
00	40	80	600	V	cast	1723.4	1779.6	1923.2

The plain concrete specimens were cast first. Next, the remaining concrete volume in the drum was calculated, and the weight of the fibres corresponding to a fibre dosage of 40 kg/m<sup>3</sup> was gradually added to the rear of the mixer and then thoroughly mixed for approximately 10 minutes. To ensure the workability of the mix was not compromised by the addition of the fibres to the concrete, some superplasticizer was added to the concrete while the fibres were being mixed into the concrete. This was done to minimize the vibration need of the SFRC during casting.

Prior to casting the SFRC specimens, a wheel-barrow of SFRC was poured and visually examined to verify balling of the fibres had not occurred, and a check was made to ensure that the fibres appeared to be uniformly distributed within the concrete.

Furthermore, the workability of all three concrete mixes was measured via a slump test (500, 520 and 355 mm for the plain concrete, 40 and 80 kg/m<sup>3</sup> SFRC mixes respectively).

With these quality controls satisfied, the first batch of SFRC specimens ( $\rho_f = 40 \text{ kg/m}^3$ ) were cast. Similarly, once the 40 kg/m<sup>3</sup> specimens were cast, the same procedure was repeated to batch and cast the SFRC mix containing 80 kg/m<sup>3</sup> of fibres.

All specimens were cast in lubricated timber formwork. With exception of the three larger sizes of the plain concrete cubes (300<sup>3</sup>, 424<sup>3</sup>, and 600<sup>3</sup> mm<sup>3</sup>), which were vibrated with an immersed vibration needle, all other specimens were mounted and cast on a vibrating table. To ensure a uniform degree of compaction amongst all specimens, mobile external vibrators were also attached to the

300<sup>3</sup>, 424<sup>3</sup>, and 600<sup>3</sup> mm<sup>3</sup> fibre-reinforced specimens. Care was taken to ensure over-compaction did not occur which would otherwise lead to a non-uniform distribution of the fibres through the depth of the section. The casting surface of all specimens was ground to ensure coplanar surfaces for load introduction.

For the smaller specimen sizes (75<sup>3</sup>, 106<sup>3</sup> and 150<sup>3</sup> mm<sup>3</sup>), additional specimens were cut out from a larger cuboid to study the influence of any wall effects on the fibre orientation.

The three theoretical fibre contents were: 0, 40 and 80 kg/m<sup>3</sup>. The actual fibre content was determined by extracting samples (cylinders 150 mm diameter by 300 mm high) of fresh SFRC. The cylinders were emptied, the cementitious content washed out and the fibres extracted using a magnet. The fibres were then dried and their weight measured. While the higher fibre dosage mix was found to have consistent fibre dosages with respect to the theoretical value ( $\pm 6\%$ ), the mix with the lower dosage of fibres displayed a much higher degree of scatter ( $\pm 31\%$ ).

The specimens were tested in ascending order with respect to their size. Testing began at an age of 20 days and testing of all specimens took place over a period of 7 days. The mechanical properties of the concrete (cylinder compressive strength  $f_c$ , modulus of elasticity  $E_c$  and tensile strength  $f_{ct}$ ) were determined at day 24 of the experimental campaign. These results are summarized in Table 2. The tensile strength was obtained by means of the conventional cylindrical double punch tests as proposed by Chen [4]:

$$f_{ct} = \frac{4N_{cr}}{\pi(2.4Dh - p^2)} \quad (1)$$

where  $N_{cr}$  is the cracking load of the specimen,  $D = 150$  mm and  $h = 150$  mm corresponding to the cylinder diameter and height, respectively, and  $p = D/4$  is the punch diameter. Additionally, to characterise the residual tensile strength offered by the SFRC, four 3-point bending tests according to EN 14651 [12] were performed on each of the 40 and 80 kg/m<sup>3</sup> mixes; these results are reported in Table 3.

**Table 2:** Mechanical properties of the concrete mixes (mean value and coefficient of variation).

$\rho_f$ [kg/m <sup>3</sup> ]	$f_c$ [MPa]	$E_c$ [GPa]	$f_{ct}$ [MPa]
0	38.6 ( $\pm 1.8\%$ )	32.8 ( $\pm 3.4\%$ )	3.24 ( $\pm 1.5\%$ )
40	39.2 ( $\pm 1.5\%$ )	31.6 ( $\pm 2.5\%$ )	3.19 ( $\pm 3.1\%$ )
80	43.9 ( $\pm 1.4\%$ )	32.5 ( $\pm 0.9\%$ )	3.64 ( $\pm 3.0\%$ )

**Table 3:** Residual flexural tensile strength from 3-point bending tests (mean value and coefficient of variation).

$\rho_f$ [kg/m <sup>3</sup> ]	$f_L$ [MPa]	$f_{R1}$ [MPa]	$f_{R2}$ [MPa]	$f_{R3}$ [MPa]	$f_{R4}$ [MPa]
40	4.59 ( $\pm 7.2\%$ )	5.05 ( $\pm 20.2\%$ )	5.31 ( $\pm 20.3\%$ )	4.75 ( $\pm 14.5\%$ )	4.29 ( $\pm 15.4\%$ )
80	4.54 ( $\pm 7.9\%$ )	6.17 ( $\pm 18.0\%$ )	6.30 ( $\pm 14.8\%$ )	6.07 ( $\pm 15.5\%$ )	5.91 ( $\pm 15.1\%$ )

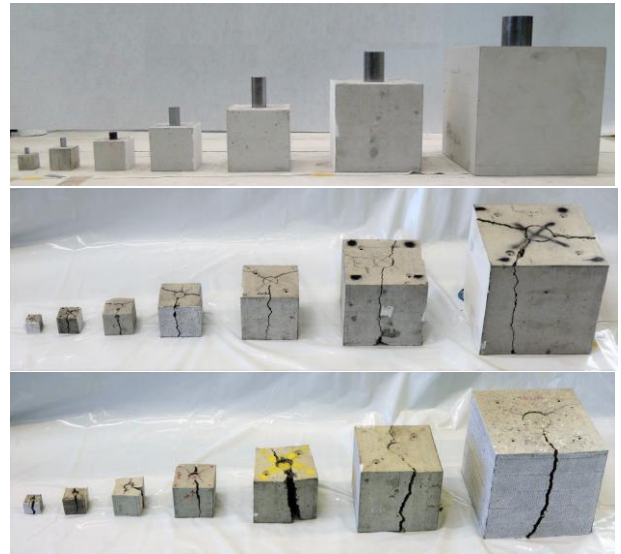


**Figure 2:** (a) Specimens before testing; (b) plain concrete and (c) SFRC specimens ( $\rho_f = 40$  kg/m<sup>3</sup>) after testing

### 2.3 Test setup and protocol

For every combination of fibre content and specimen size, two specimens were tested. One specimen was loaded in the direction of casting (denoted as “V” for “vertical”) while its twin was loaded in the lateral direction with respect to its casting direction (designated “H” for “horizontal”). Similar to what was initially

proposed by Chen [4], the diameter of the steel punches used to apply load to the specimen was one-quarter of the side length of the cube (see Figure 1). The punches were carefully centred on the loading surfaces of the cubes to minimize applied eccentricities. The specimens were loaded in ram displacement control. The initial rate of the applied displacement until cracking was chosen to obtain a stress increase in the punch of roughly 0.5 MPa/s. After cracking, the speed was adjusted according to the following scheme (ram displacement after cracking):

*cubes of 75 and 106 mm*

- 0 – 0.5 mm      0.1 mm/min

- > 0.5 mm      0.5 mm/min

*cubes larger than 106 mm*

- > 0 mm      0.5 mm/min

The test was terminated at a loss of around 80% of the peak load or at a maximum ram displacement of 15 mm, whichever occurred first.

Aside of the ram displacement and the force signal from the testing machine, 3D motion capture tracking with optical markers by NDI Measurement Sciences were used to assess the displacement of the punches for the effective penetration into the concrete. Furthermore, optical markers were also placed on two faces of each cube. The other two faces were provided with a speckle pattern in order to track surface displacements with a three-dimensional digital image correlation measurement system. The correlation was conducted using the VIC-3D software by Correlated Solutions. The measurements on the cube faces will be used to directly assess the crack kinematics, which is currently in progress.

### 3 RESULTS

First results of the experimental campaign are presented in the following.

#### 3.1 General behaviour pre and post cracking

When a concentrated load is applied over a limited area of concrete, the compressive

stresses disperse within the concrete. As a consequence of the dispersion of stresses below the two punches in a double punch test, radial and circumferential bursting tensile stresses develop within the specimen. These stresses increase approximately in proportion with the applied load until the maximum tensile stresses in the concrete reach the material strength, where cracking occurs. At this point, a conical fragment materialises beneath each steel punch, and vertical cracks propagate radially from these across the specimen. As the conical fragments penetrate the concrete at increasing displacements, the outer concrete segments displace in the radial direction. Hence, while a sliding failure takes place along the edges of the conical fragments, separation failure between the outer fragments is dominating the response [5]. For quasi-brittle materials such as plain concrete, cracking essentially corresponds to failure, which is of a brittle nature with an abrupt and pronounced drop in its load bearing capacity. For materials having a substantial post cracking strength, such as SFRC, a smoother strain softening or even toughening behaviour is expected.

In all plain-concrete specimens tested in this study, three vertical radial cracks formed as schematically illustrated in Figure 1b and visible in Figure 2b. Although in many of the SFRC cubes three main radial cracks developed, some specimens displayed up to 5 cracks after the onset of cracking.

With increasing penetration of the punches, which corresponds to an increase of crack width, the circumferential displacement in the SFRC specimens tends to localize in the weakest radial crack plane (as seen in Figure 2c).

#### 3.2 Definition of nominal stress

Size effect can be understood as the dependence of structural strength (pre- or post-cracking) on the characteristic structure's size  $s$  when geometrically similar structures made of the same material are compared [13]. In this paper, we define a nominal stress as follows:

$$\sigma_N = \beta \frac{N}{s^2} \quad (2)$$

The coefficient  $\beta$  in Eq. (2) is constant for geometrically similar structures and in this paper is chosen in such a way that  $\sigma_N$  at cracking for a specimen size corresponding to that of the standard cylindrical double-punch test (i.e.  $s = 150$  mm) equals the tensile strength of concrete  $f_{ct}$  given by Eq. (1), with  $D = 150$  mm,  $h = 150$  mm, and  $p = D/4$ . By this definition, we obtain  $\beta = 0.54$ . We note that  $\sigma_N$  has no real physical meaning; any arbitrary value of  $\beta$  can be chosen and won't influence the conclusions about size effect stated in the following. By the definition set above, in the following, we describe the size effect as the variation of  $\sigma_N$  with respect to the structure size  $s$ .

### 3.3 Cracking load

Table 1 reports the cracking load of each specimen.

As shown by Marti [5], Bažant's nonlinear fracture mechanics-based relationship [7] adequately captures the size effect seen in plain concrete double punch cylinder tests. In this approach, Bažant suggests that limit analysis and linear elastic fracture mechanics (LEFM) apply for very small and very large specimen sizes, respectively. For intermediate sizes, a smooth transition between the two theories applies. Bažant's size-effect relationship may be written as:

$$\bar{\sigma}_{N,cr} = \frac{f_{ct}}{\sqrt{1 + \frac{s}{\lambda D_{\max}}}} \quad (3)$$

where  $\bar{\sigma}_{N,cr}$  is the prediction for the nominal stress defined in Eq. (2) and  $\lambda$  is an empirical constant. For  $s = 0$ , Eq. (3) yields  $\bar{\sigma}_{N,cr} = f_{ct}$ , while for very large values of  $s$ ,  $\bar{\sigma}_{N,cr}$  is inversely proportional to  $\sqrt{s}$  as suggested by LEFM.

To compare the cracking load for the different specimen sizes, the nominal stress at the onset of cracking  $\sigma_{N,cr}$  is evaluated

according to Eq. (2) for each test with  $\beta = 0.54$ . Eq. (3) is transformed to  $1/\sigma_{N,cr}^2 = a + b s/D_{\max}$  which is fitted to the test data by linear regression. This yields two constants  $a$  and  $b$ ; based on Eq. (3),  $f_{ct} = 1/\sqrt{a}$  and  $\lambda = a/b$ . The values of the two smallest specimen sizes ( $s = \{75 \text{ mm}, 106 \text{ mm}\}$ ) lie much lower than would be expected; this is most probably due to the fact that these specimens are so small (less than 7 times the maximum aggregate size, and approximately three times the fibre length) and as such cannot be considered representative for a volume element. This reasoning is supported by the fact that the cubes cut out of a larger concrete block (where the wall/boundary effect is effectively removed) fit much better with the tendencies of the test data. For this reason, the two smallest sizes were not considered in the regression analysis. The optimal fitting parameters are plotted in Figure 3. It is evident that there is a pronounced size effect, which is in good agreement with Bažant's relationship Eq. (3).

Comparing the nominal stresses at cracking without fibres (Figure 3a) with those with fibres (Figure 3b and Figure 3c), it can be concluded that the steel fibres have no clear influence on the size effect of the cracking load. However, for the SFRC specimens, there is a clear difference in the responses with respect to the loading vs. casting directions. For the specimens where the load was applied in the vertical (casting) direction, a significantly higher cracking load was seen when compared to the specimens tested in the horizontal direction. This difference can be explained by the preferentially horizontal orientation of the fibres caused by the filling process, and / or the applied vibration on the concrete matrix during casting, causing slightly different properties of the concrete matrix in the horizontal and vertical directions. Such differences influence the crack formation process and subsequently the cracking load, and in addition, the post-cracking behaviour of the SFRC cubes (which will be discussed in following section).

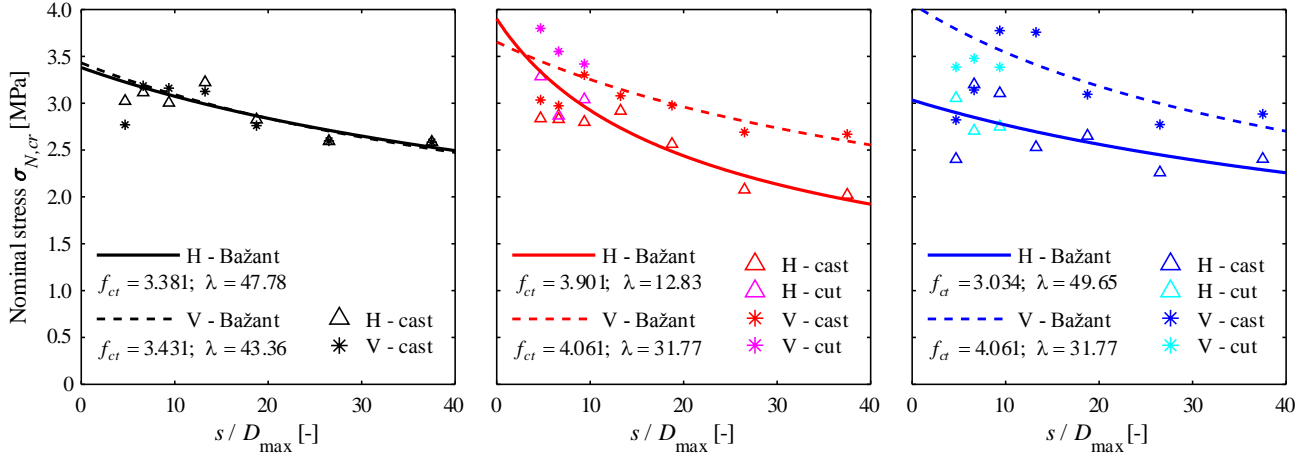


**Figure 3:** Effect of specimen size on nominal stress at cracking for (a) plain concrete; (b) fibre content of  $\rho_f = 40$  kg/m<sup>3</sup> and (c) fibre content of  $\rho_f = 80$  kg/m<sup>3</sup>.

### 3.3 Load – penetration behaviour

Although the fibres are apparently unable to mitigate the size effect seen in the cracking load of the specimens, the presence of the fibres had a significant impact on the post-cracking residual behaviour of the concrete cubes. The post-cracking behaviour of the SFRC specimens is shown in Figure 4 and Figure 5 respectively for the two fibres contents. In these plots, the penetration represents the combined penetration of the upper and the bottom punches into the cubes, while the nominal stress  $\sigma_N$  is that defined by Eq. (2).

The results presented in Figure 4 and Figure 5 show a pronounced material anisotropy. The post-cracking strength of the specimens tested in the vertical direction is significantly higher than the strength of the specimens tested in the horizontal direction for all tested sizes. This result is most readily explained by a non-homogenous distribution and orientation of the fibres. Steel fibres have been found to align with the flow of concrete [14]. In this case, the fibres tended to orientate parallel to the casting surface, and this alignment is probably exacerbated due to the applied vibration. A preliminary visual inspection on the specimens suggests that in the vertical tests, the separation cracks had a larger amount of fibres bridging the cracks than the horizontal tests. In this respect, multidirectional double punch tests have been very effective to evaluate the

influence of fibre orientation, and this finding supports those by Pujadas [3].

A consistent analysis of the post-cracking size effect of SFRC would require the analysis of the crack kinematics, which is beyond the scope of this paper. Only a preliminary evaluation can be made based on the comparison of the nominal stress versus penetration curves for different size specimens, assuming that the punch penetration correlates to the total circumferential crack opening displacement [15]. This preliminary evaluation is illustrated in the bottom right plots presented in Figure 4 and Figure 5 for the tests loaded in the vertical direction.

It can be seen that the smaller specimens exhibit a more pronounced softening with respect to the punch penetration, which may, however, be more related to the wall/boundary effect rather than a “negative” size effect on the local crack opening-tensile stress response. On the other hand, the post-peak branches of the larger specimens are very similar, indicating a size independent crack opening-tensile stress response, which however, when normalizing the displacements with respect to the specimen size, translates to a markedly more pronounced softening with increasing specimen size. These effects are currently being investigated by the authors.

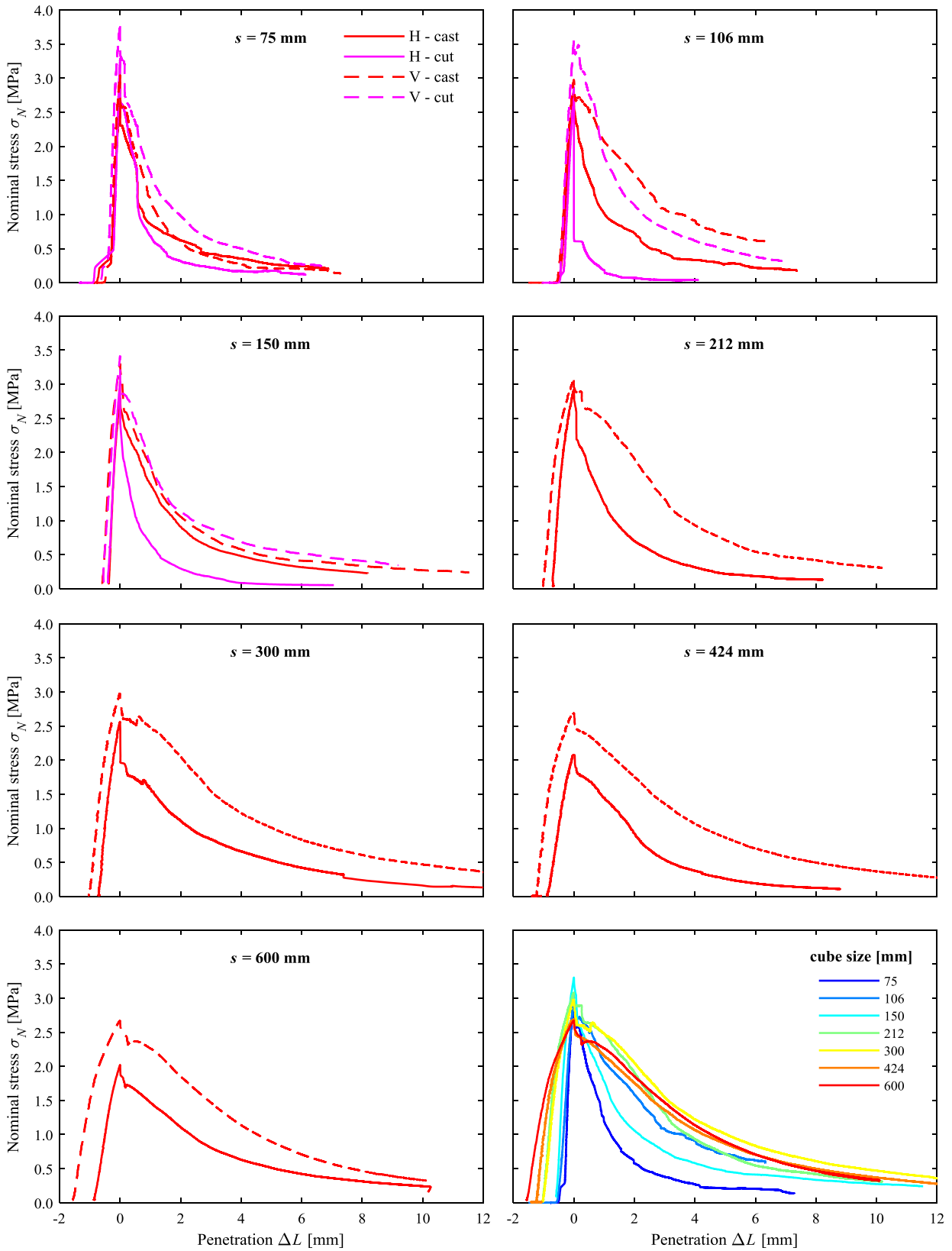


**Figure 4:** Nominal stress  $\sigma_N$  vs. penetration of FRC specimens ( $\rho_f = 40 \text{ kg/m}^3$ ).

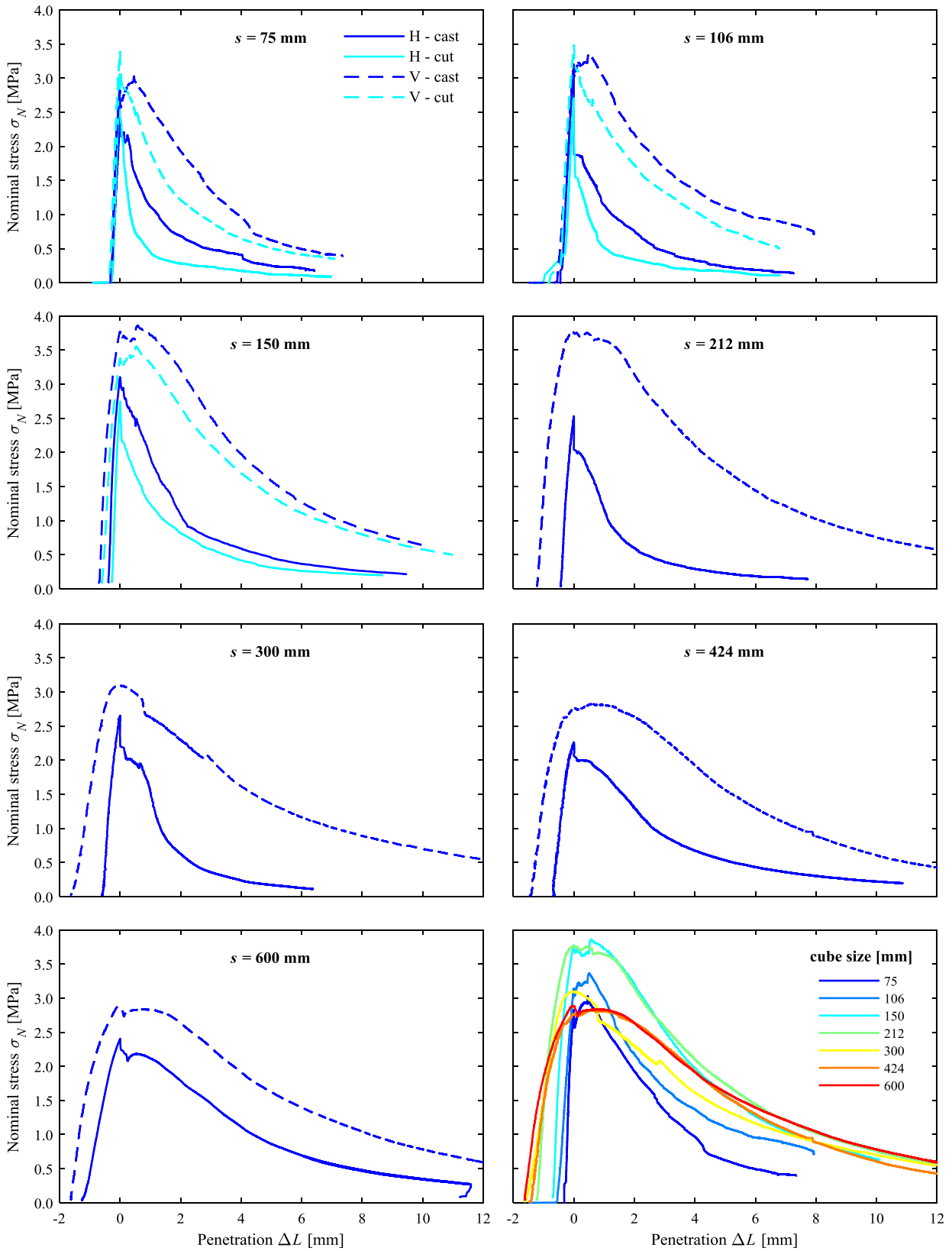


**Figure 5:** Nominal stress  $\sigma_N$  vs. penetration of FRC specimens ( $\rho_f = 80 \text{ kg/m}^3$ ).

#### 4 CONCLUSIONS AND OUTLOOK

This paper presents preliminary results of a study investigating the effect of specimen size on the response of multi-directional double punch tests on SFRC cubes of varying sizes ( $75^3$  to  $600^3$  mm<sup>3</sup>). It was found that these tests are a simple and effective method to experimentally assess a range of influences including specimen size, loading direction, and wall (boundary) effects in SFRC. The specimens are relatively easy to prepare, and the testing procedure can be readily standardised.

The loading direction was seen to have a substantial influence on the cracking load as well as the nominal stress in the post-cracking range of testing. Specimens which were loaded in the vertical (casting) direction were able to carry higher nominal stresses particularly after cracking, which might be attributed to a predominantly horizontal fibre orientation as a result of the flow and vibration of the SFRC during casting of the specimens.

A clear size effect was observed on the cracking load for all concretes, regardless of fibre content. These results generally support the size effect model of Bažant [7]. Regarding the size effect on the post-cracking behaviour, only a preliminary evaluation was possible based on the punch penetration, allowing no final conclusions. More refined analyses of this aspect, accounting for the crack kinematics, are currently being carried out by the authors.

#### 5 ACKNOWLEDGEMENTS

The experiments described in this paper were carried out as a part of the Master's Projects of Sina Fehr and Simon Karrer at ETH Zurich, whose contributions are greatly acknowledged.

#### REFERENCES

[1] W. Kaufmann, A. Amin, A. Beck, and M. Lee, 'Shear transfer across cracks in steel fibre reinforced concrete', *Engineering Structures*, vol. 186, pp. 508–524, May 2019.

- [2] A. Amin, S. J. Foster, R. I. Gilbert, and W. Kaufmann, 'Material characterisation of macro synthetic fibre reinforced concrete', *Cement and Concrete Composites*, vol. 84, pp. 124–133, Nov. 2017.
- [3] P. Pujadas, A. Blanco, S. H. P. Cavalaro, A. de la Fuente, and A. Aguado, 'Multidirectional double punch test to assess the post-cracking behaviour and fibre orientation of FRC', *Construction and Building Materials*, vol. 58, pp. 214–224, May 2014.
- [4] W. F. Chen, 'Double Punch Test for Tensile Strength of Concrete', *ACI Journal*, vol. 67, no. 12, pp. 993–995, 1970.
- [5] P. Marti, 'Size Effect in Double-Punch Tests on Concrete Cylinders', *MJ*, vol. 86, no. 6, pp. 597–601, Nov. 1989.
- [6] C. Molins, A. Aguado, and S. Saludes, 'Double Punch Test to control the energy dissipation in tension of FRC (Barcelona test)', *Materials and Structures*, vol. 42, no. 4, pp. 415–425, May 2009.
- [7] Z. P. Bažant and J. Planas, *Fracture and size effect in concrete and other quasibrittle materials*. Boca Raton: CRC Press, 1998.
- [8] J. G. M. van Mier, *Concrete fracture: a multiscale approach*, First issued in paperback. Boca Raton London New York: CRC Press, Taylor & Francis Group, 2017.
- [9] K. Noghabai, 'Beams of Fibrous Concrete in Shear and Bending: Experiment and Model', *Journal of Structural Engineering*, vol. 126, no. 2, pp. 243–251, Feb. 2000.
- [10] H. H. Dinh, G. J. Parra-Montesinos, and J. K. Wight, 'Shear Behavior of Steel Fiber-Reinforced Concrete Beams without

Stirrup Reinforcement’, *SJ*, vol. 107, no. 5, pp. 597–606, Sep. 2010.

*Mechanics (Ingenieur Archiv)*, vol. 69, no. 9–10, pp. 703–725, Nov. 1999.

[11] F. Minelli, A. Conforti, E. Cuenca, and G. Plizzari, ‘Are steel fibres able to mitigate or eliminate size effect in shear?’, *Materials and Structures*, vol. 47, no. 3, pp. 459–473, Mar. 2014.

[14] P. Stähli, R. Custer, and J. G. M. van Mier, ‘On flow properties, fibre distribution, fibre orientation and flexural behaviour of FRC’, *Materials and Structures*, vol. 41, no. 1, pp. 189–196, Jan. 2008.

[12] ‘DIN EN 14651:2007-12, Prüfverfahren für Beton mit metallischen Fasern\_ - Bestimmung der Biegezugfestigkeit (Proportionalitätsgrenze, residuelle Biegezugfestigkeit); Deutsche Fassung EN\_14651:2005+A1:2007’, Beuth Verlag GmbH.

[15] P. Pujadas, A. Blanco, S. Cavalaro, A. de la Fuente, and A. Aguado, ‘New Analytical Model to Generalize the Barcelona Test Using Axial Displacement’, *Journal of Civil Engineering and Management*, vol. 19, no. 2, pp. 259–271, Apr. 2013.

[13] Z. P. Bažant, ‘Size effect on structural strength: a review’, *Archive of Applied*